ARL-MR-1117 ● Dec 2024

Development of a Sprague Dawley Computational Surrogate

by Brian Fagan, Erika Matheis, Carey Balaban, Marianne Cites, and Christopher Dumm

NOTICES

Disclaimers

The findings in this report are not to be construed as an official Department of the Army position unless so designated by other authorized documents.

Citation of manufacturer's or trade names does not constitute an official endorsement or approval of the use thereof.

Destroy this report when it is no longer needed. Do not return it to the originator.

ARL-MR-1117 ● DEC 2024

Development of a Sprague Dawley Computational Surrogate

Brian Fagan and Carey Balaban
DEVCOM Army Research Laboratory

Erika Matheis
SURVICE Engineering

Marianne Cites and Christopher Dumm
University of Pittsburgh

REPORT DOCUMENTATION PAGE

1. REPORT DATE	2. REPORT TYPE	3. DATES COVERED	
		START DATE	END DATE
December 2024	Memorandum Report	7/31/2023	10/30/2024

4. TITLE AND SUBTITLE
Development of a Sprague Dawley Computational Surrogate

5a. CONTRACT NUMBER	5b. GRANT NUMBER	5c. PROGRAM ELEMENT NUMBER
5d. PROJECT NUMBER	**5e. TASK NUMBER**	**5f. WORK UNIT NUMBER**

6. AUTHOR(S)
Brian Fagan, Erika Matheis, Carey Balaban, Marianne Cites, and Christopher Dumm

7. PERFORMING ORGANIZATION NAME(S) AND ADDRESS(ES)	8. PERFORMING ORGANIZATION REPORT NUMBER
DEVCOM Army Research Laboratory ATTN: FCDD-RLA-TB Aberdeen Proving Ground, MD 21005	ARL-MR-1117

9. SPONSORING/MONITORING AGENCY NAME(S) AND ADDRESS(ES)	10. SPONSOR/MONITOR'S ACRONYM(S)	11. SPONSOR/MONITOR'S REPORT NUMBER(S)

12. DISTRIBUTION/AVAILABILITY STATEMENT
DISTRIBUTION STATEMENT A. Approved for public release: distribution unlimited.

13. SUPPLEMENTARY NOTES
ORCID: Erika Matheis, 0000-0002-5122-1503

14. ABSTRACT
This report presents the development of a 3D computational surrogate for a Sprague Dawley rat. We outline the steps taken from procurement of medical scan images to finalized geometry.

15. SUBJECT TERMS
anatomical modeling, 3D modeling, model development, Sprague Dawley rat, Biological and Biotechnology Sciences

16. SECURITY CLASSIFICATION OF:			17. LIMITATION OF ABSTRACT	18. NUMBER OF PAGES
a. REPORT	b. ABSTRACT	C. THIS PAGE		
UNCLASSIFIED	UNCLASSIFIED	UNCLASSIFIED	UU	18

19a. NAME OF RESPONSIBLE PERSON	19b. PHONE NUMBER *(Include area code)*
Brian Fagan	(410) 278-3841

STANDARD FORM 298 (REV. 5/2020)
Prescribed by ANSI Std. Z39.18

Contents

List of Figures

List of Tables

1. Introduction and Background

Computation surrogates provide a useful way to explore and understand a wide variety of multi-physic responses (e.g., mechanical response and thermal response). Sprague Dawley rats are an outbred rat strain commonly used in biomedical research. It was created from a cross of a Wistar rat with another rat strain. However, currently available Sprague Dawley models seem to be lacking detailed inner ear representations.

This report presents the development of a 3D computational surrogate for a Sprague Dawley rat. The steps taken from procurement of medical scan images to finalized geometry are outlined.

2. Method

The development process used for this 3D anatomical rodent model reconstructed from medical images can be divided into four steps: imaging, segmentation, geometry cleanup and merging, and simplifying the geometric surfaces.

2.1 Computed Tomography Imaging

In this report, we present computed tomography (CT) images in the development of the rodent model. We also used scans with three separate resolutions. Four female Sprague Dawley sentinel rats from the animal colony (fresh cadavers) were scanned at 100- and 250-µm resolution using a Vimago GT30 made by Epica Animal Health (Landrum, SC). The rats ranged from approximately 260 to 290 g. The field of view for the lower resolution scan focused on the entire rat body, whereas the field of view for the higher resolution scan focused on the head (Figure 1). As previously stated, the primary focus for this model development effort was focused on the head of the rat.

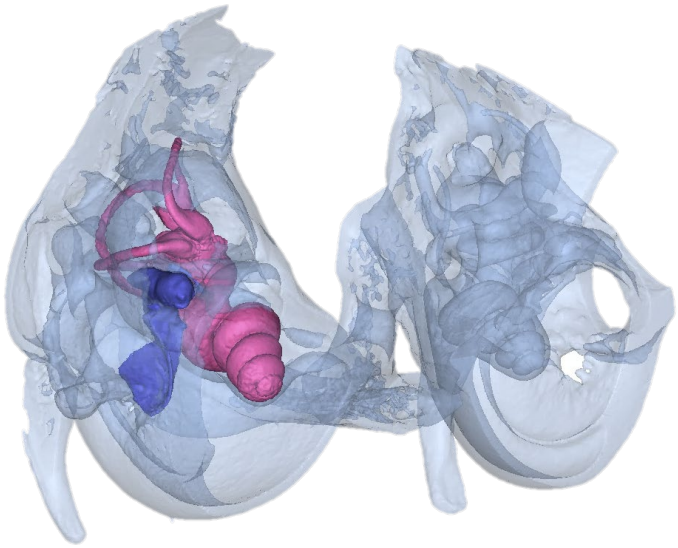

Figure 1. Reconstruction of the skull base, middle ear, and inner ear from the µCT scan of the skull.

Even the 100-µm resolution was insufficient to resolve some anatomical features in the head. These features were manually reconstructed; the process will be discussed later in this report. However, because it was critical to accurately capture the inner ear for this program, a rat skull was also scanned, via µCT, to resolve the intricate geometry. The skull was scanned with a Bruker SkyScan1272 X-ray microscope system equipped with a complementary metal–oxide–semiconductor (CMOS) detector. Nominal resolution (pixel size) due to standoff and sample size was 10.5 µm. A stock 0.11-mm copper filter was used at an applied X-ray tube voltage of 100 kV. A camera pixel binning of 2 × 2 was applied. The scan orbit was 180° with a rotation step of 0.2°.

Reconstruction of the scan was carried out with a modified Feldkamp algorithm using the SkyScan NRecon software accelerated by graphics processing unit. Ring artifact correction of 5 and beam hardening correction of 7% were used.

2.2 Segmentation

Materialise Mimics (version 26, Materialise NV, Leuven, Belgium) was used to view and upload the DICOM (Digital Imaging and Communications in Medicine) images from the CT scans. CT distinguishes different density values in Hounsfield units (HUs) where different tissue types are separated via differences in density. The densities that are captured range from –1024 to 3071, where more dense materials (like bone) have a higher value. Anatomic parts of the Sprague Dawley model were segmented through thresholding HU values for the low-resolution scan (Table 1).

Table 1. HU value ranges for low-resolution scan of different anatomic parts.

Anatomic part	Density range (HUs)	
	Low	High
Brain	1128	2083
Bone	1553	3071
Soft tissue	48	1700
Eyes	1301	3071
Airways	–1024	325
Lungs	–1024	325
Heart	313	1337
Liver	–1024	−982
Kidneys	1156	1421
Diaphragm	–964	839
Peritoneal cavity	–1000	1421

If the masks overlapped, they were segmented by using the split mask function that separates touching entities by manually marking the desired regions of interest as shown in Figure 2. Further editing of the mask may have been done manually to segregate parts through the edit masks function with lassoing and then applying a region grow function. Once masks were generated for all anatomic parts listed in Table 1, the Boolean function was applied to make sure there was no overlap on masks. Three-dimensional parts were then generated through the *calculate part* function, with optimal settings where the part is not reduced nor averaged in intensity. These parts were then exported into an STL file format for further model development.

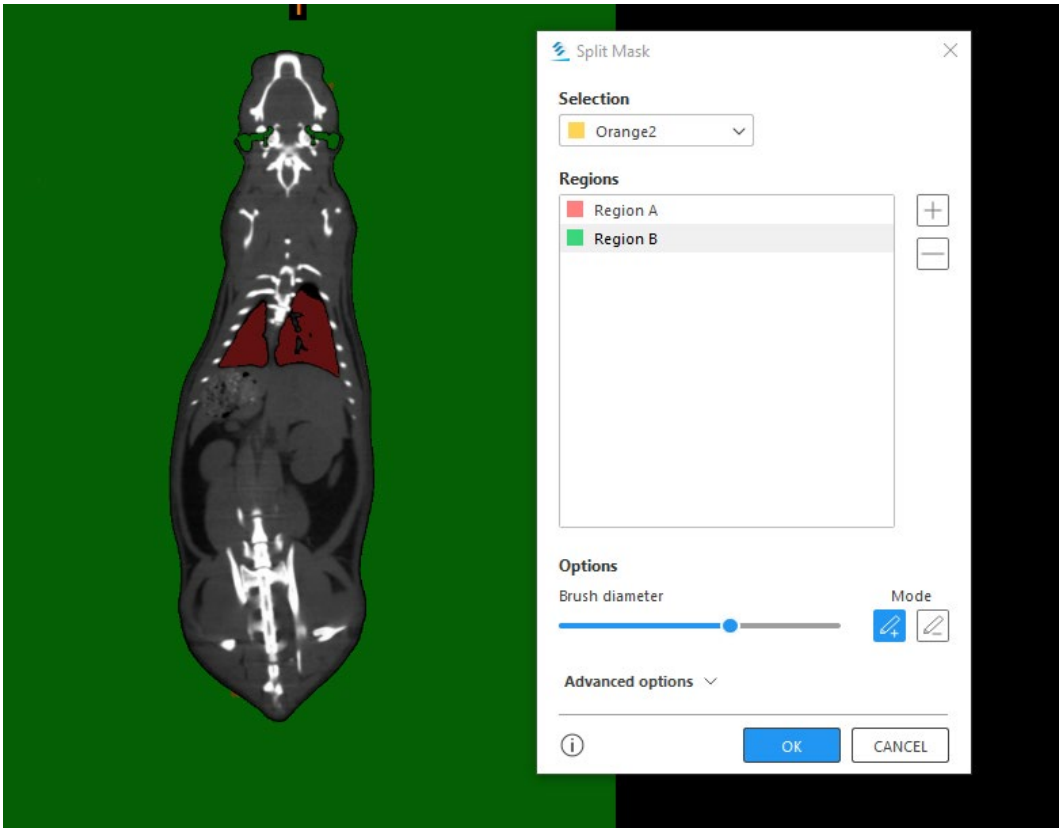

Figure 2. An example of splitting an overlapping threshold where two masks would be created. Region A (red) is selected for the lungs and Region B is selected for the air within the chamber (green).

For the high-resolution scan, which encompassed the head region, the density ranges used were different than the low-resolution scan because each scan may have slightly different density values based on the averaging of each pixel. The smaller pixel size for the high-resolution scan is one factor that contributes to values that differ from the lower resolution scan. The density ranges for the high-resolution scan are in Table 2.

Table 2. Hounsfield unit value ranges for high-resolution scan of different anatomic parts.

Anatomic part	Density range (HUs)	
	Low	High
Brain	1036	1891
Bone	2662	3071
Eyes	1457	1891
Airway	–1024	819
Ear canals	–1024	819

The same process was used to mask the high-resolution scan as that for the low-resolution scan. Parts were created from the masks through the *calculate part* function. Files in STL format were created for further model development in other

software. The high-resolution scan offers more detail for anatomic parts that are particularly important for emerging research, and the low-resolution scan offers a full picture of the animal model.

2.3 Editing (Cleaning Up) Segmented Surface Geometry

The surfaces produced through the segmentation process required some manual modification and editing ("clean up") to remove artifacts. This came in the form of three broad categories: merging segmentations of different resolutions, reconstruction of anatomical details, and general fixes and cleanup to the geometry. These processes were completed in Blender (version 3.2).

First, a couple of features located in the head region needed to be manually reconstructed. The resolution of the scans was insufficient to accurately capture these features in the model. They included the auditory bullae (Figure 3) and portions of the base of the skull (Figures 4 and 5). This process consisted of creating additional surfaces at the approximate positioning of the bone from images of rat skulls. Additional features that were constructed as part of this process include the soft tissue of the ears and the round and oval windows of the inner ears.

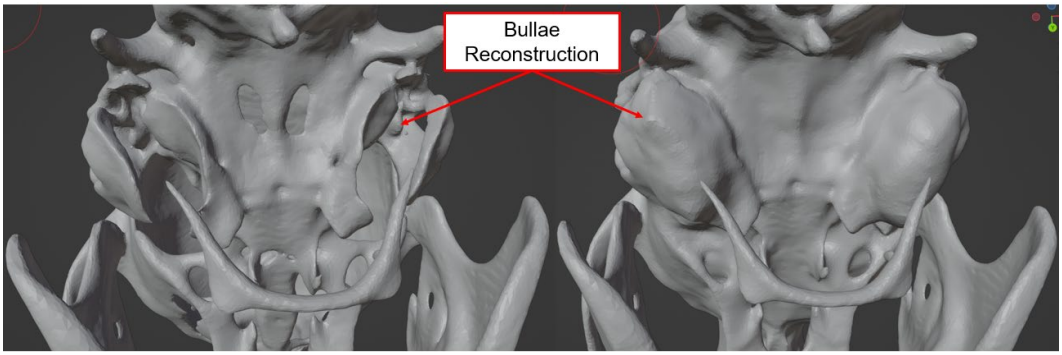

Figure 3. Manual reconstruction of auditory bullae: (left) pre-reconstruction and (right) reconstructed bullae.

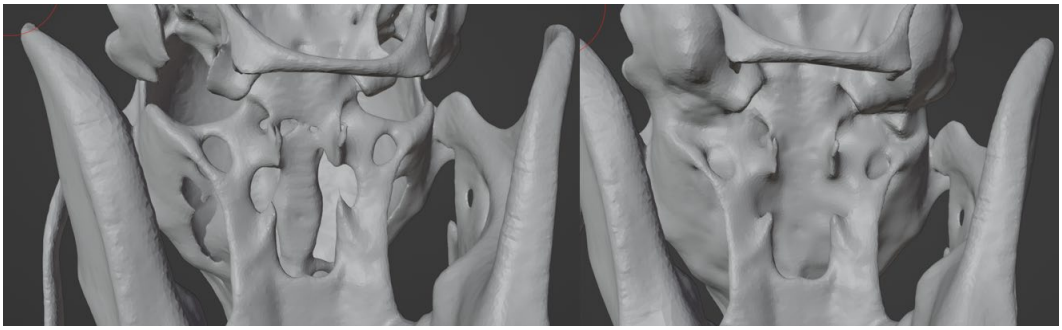

Figure 4. Manual reconstruction of skull base. Inferior side view: (left) pre-reconstruction and (right) reconstructed.

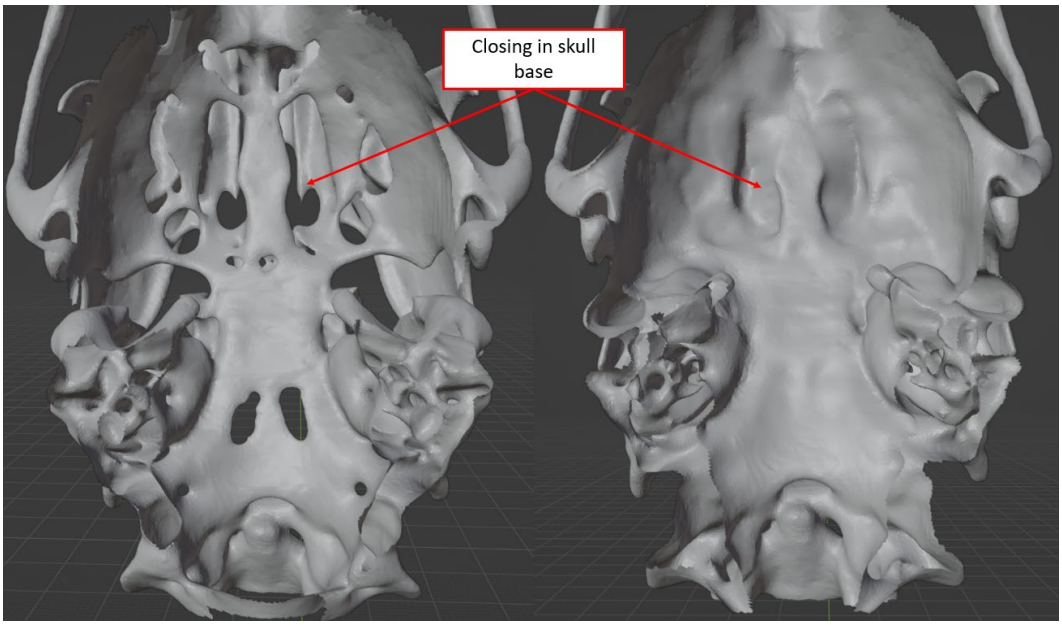

Figure 5. Manual reconstruction of skull base. Superior side view: (left) pre-reconstruction and (right) reconstructed.

The second cleanup step was merging the surfaces from the segmentations of the CT scans of different resolutions. The merger of the 250- and 100-µm surfaces was straightforward since the scans were taken consecutively from the same rat in the same orientation (Figures 6 and 7). The surfaces were spliced together, and smoothing operations was applied to the interface. The sizes of the STL facets were made more uniform between the two previous surfaces by these operations (Figure 6). Merging in the inner ear surfaces segmented from the 10-µm resolution scans required some additional steps since the scan was from a different rat than the other two scans. The inner ear was positioned and scaled to fit appropriately at the petrosal bones of the skull. Using Blender's sculpt feature, the petrosal bone surface was slightly modified to fully encapsulate the inner ear.

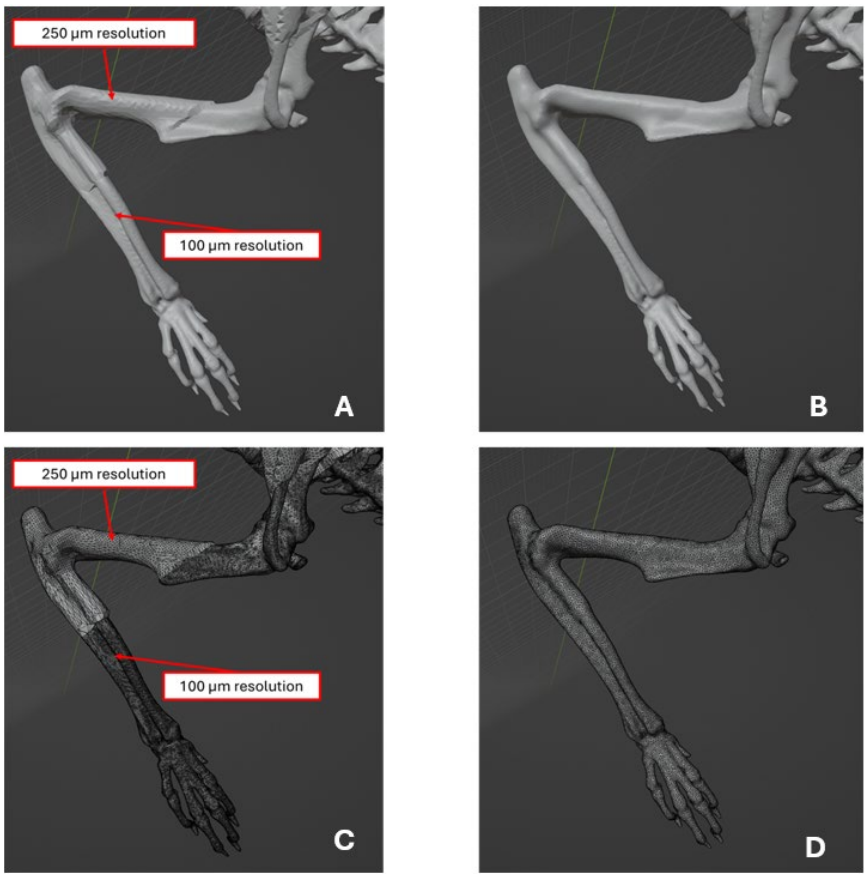

Figure 6. Merger of segmented surfaces from the 100- and 250-µm resolution CT scans (A) pre-merging, (B) post-merger, (C) pre-merging with surface edges displayed, and (D) post-merger with surface edges displayed.

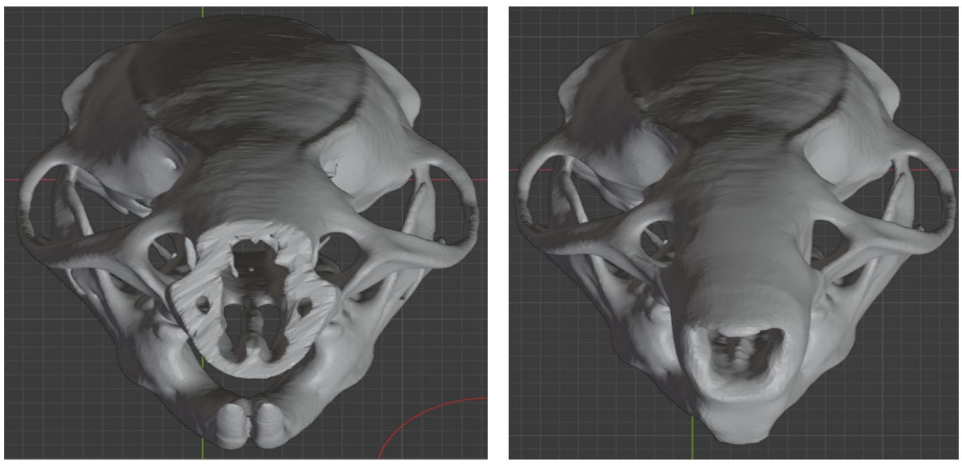

Figure 7. Merger of segmented surfaces from the 100- and 250-µm resolution CT scans of skull (left) pre-merger and (right) post-merger.

Finally, several generic alterations and fixes were made to the surfaces. They included removing all non-manifold facets and internal facets from the

segmentation process, smoothing the surface to remove spikes, and using Blender's sculpt feature to make the facet size near uniform on each surface.

2.4 Reconstructing Faceted Surfaces with NURBS Surfaces

The finalized faceted surfaces had ~1,800,000 facets in total. For some of the applications for which these models are planned to be used, the surfaces were deemed to have too many facets. Geomagic Wrap 2021 was used to reduce the total number of surfaces by converting the faceted geometry to non-uniform rational basis spline NURBS surfaces. An example of the results of this process are illustrated in Figure 8, which shows the reduction in the number of surfaces in the lungs. The starting number of faceted surfaces was 37,754 and was reduced to 548 NURBS surfaces. These new parts consisted of ~53,000 surfaces in total. Boolean operations were then applied to the surfaces to make volumes with matching surfaces for each anatomical part.

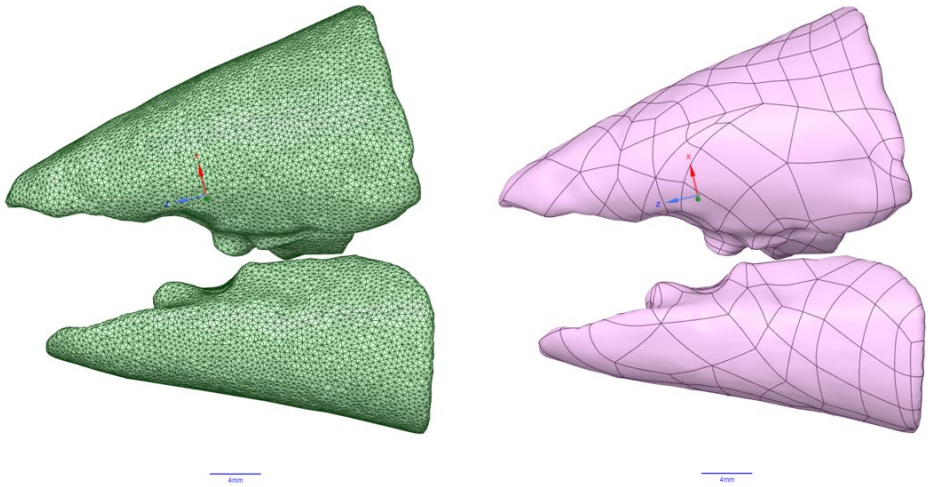

Figure 8. Resurfacing of the lung surface using Geomagic Wrap: (left) starting STL surface and (right) final NURBS surface.

2.5 Body Overview

The final model consisted of 23 separate volumes (Figure 9). The volumes consisted of a homogenized soft tissue, skull and skeleton torso, hyoid bone, bone–arm (×2), brain, diaphragm, heart, airway, liver, abdominal cavity, eye (×2), lung (×2), kidney (×2), inner ear (×2), oval window (×2), and round window (×2).

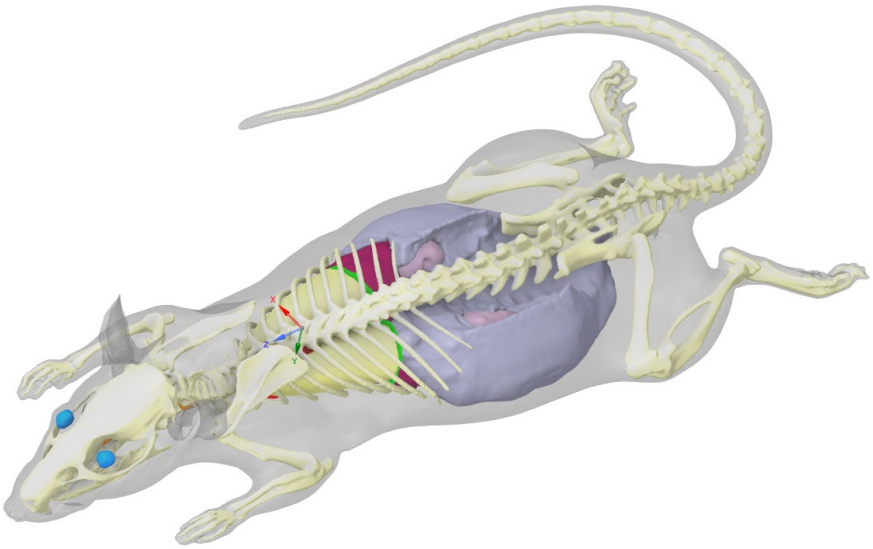

Figure 9. Sprague Dawley rat model.

2.6 Inner Ear Overview

One of the core features in this model development effort was the inclusion of a biofidelic inner ear models to meet program goals. These models were generated from segmenting out the interior of the bony labyrinths from the μCT scan of the rat skull. A thin slice of the volume was converted to represent the round window membrane, and an approximation for the stapes footplate was generated and overlayed over the oval window (Figure 10).

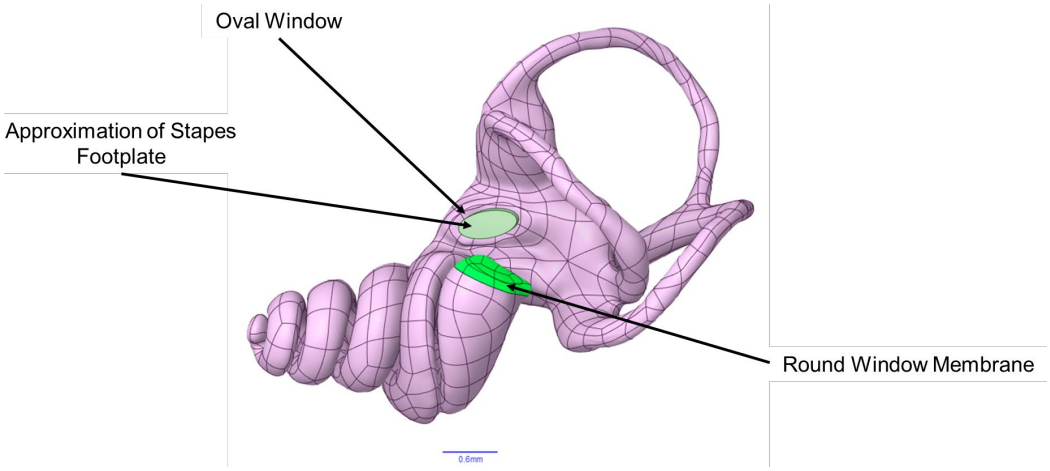

Figure 10. Sprague Dawley rat inner ear model.

The round and oval windows are exposed to the middle ear cavities, whereas the rest of the inner ears are encased in the temporal bone of the skull. The simplified representation of the stapes footplate was placed over a portion of the oval window to mimic the boundary conditions that the oval window would experience.

3. Conclusion

A 3D computational surrogate for a Sprague Dawley rat was developed and delivered. We emphasized the development of the inner ear models imbedded in the skull. The steps taken from procurement of medical scan images to finalized geometry were outlined. Additional fidelity could still be added in several regions to improve the model such as separation of muscle and fat tissue, separation of the bony labyrinth and membranous labyrinth, and the inclusion of the otolith organs. Some of these improvements are being considered for an additional version of this surrogate.

List of Symbols, Abbreviations, and Acronyms

3D	three-dimensional
CMOS	complementary metal–oxide–semiconductor
CT	computed tomography
DICOM	Digital Imaging and Communications in Medicine
HU	Hounsfield unit
NURBS	non-uniform rational basis spline

1 (PDF)	DEFENSE TECHNICAL INFORMATION CTR DTIC OCA
1 (PDF)	DEVCOM ARL FCDD RLB CI TECH LIB